Bounding surface modeling for compacted silty sand

U. D. Patil
School of Engineering, University of Guam, Mangilao, GU 96913.

M. Morvan
Clermont Université, Université Blaise Pascal, Institut Pascal, BP 10448, F-63000 Clermont-Ferrand, CNRS, UMR 6602, Institut Pascal, F-63171 Aubière, France.

A. J. Puppala, L. R. Hoyos and TV Bheemasetti
Department of Civil Engineering, University of Texas at Arlington, Arlington, Texas 76019.

ABSTRACT: One of the foremost challenges in soil modeling is to simulate post-peak softening and gradual volumetric transition from compressive to dilatant type. In this research, saturated and suction-controlled consolidated drained triaxial tests were conducted on silty sand specimens that were prepared using identical static compaction method and sheared following conventional triaxial compression stress path. The constitutive model implemented in this paper is based on the rudimentary concept of BS plasticity and is formulated under critical state framework. The essential BS model parameters are calibrated using experimental test results for predictions of compacted silty sand response in saturated (zero matric suction) and unsaturated conditions (matric suction value of 50 and 250 kPa). Simulations show that BS model can reasonably simulate the post-peak strain softening response and initial compression followed by dilational volumetric response obtained from suction-controlled CTC tests with reasonable accuracy.

1 INTRODUCTION

Ever since its successful adoption by Hilf (1956), the axis-translation technique has been widely and intensively implemented worldwide by modifying conventional triaxial test to investigate on the suction-induced response of unsaturated soil. The basis of assessment of stability of unsaturated soil is largely influenced by a combination of variation in external loading and internally induced matric suction. Matric suction arises due to capillary tension forces across air-water interface and is a function of water content. Thus, existing mechanical and hydraulic properties of soil play a key role, among others, in subsequent stress-deformation response of soil skeleton.

Among the approaches to solve problems related to unsaturated soils, some researchers consider matric suction, $(u_a - u_w)$, and the excess of total stress over air pressure, that is, net normal stress, $(\sigma_3 - u_a)$, as the relevant stress state variables in implementing the axis-translation technique (Hilf 1956; Matyas and Radhakrishna 1968; Fredlund and Morgenstern 1977), while others combine pore-air pressure and pore-water pressure together in to an equation that defines single effective stress (i.e. e.g., Bishop 1959). It has been established through experiments that volume changes induced due to imposed suction and external stress are different and that these two should be considered independently, thus making former option more appropriate than latter (Jennings and Burland 1962; Matyas and Radhakrishna 1968). This first option does not allow the continuity of equation between saturated state and unsaturated state, hence recent studies have proposed the use of suction and the enlarged effective stress as stress state variables (Karube 1988; Kohgo et al. 1993; Khalili and Khabbaz 1998; Lu and Likos 2006).

Despite significant progress pertaining to fully dry and saturated soils, efforts devoted to the development and thorough validation of Bounding Surface (BS) based theories to model the essential features of unsaturated soil behavior remain rather limited. Typically, soil specimens that are normally consolidated manifest compressive type volumetric response and strain hardening type stress-strain response upon continued shearing. Such a response can be simulated using constitutive models such as Barcelona Basic Model (i.e., BBM (Alonso et al., 1990)).

However, over-consolidated soils show initial compression followed by dilational type volumetric response and subsequent post-peak strain-softening type response, upon continued shearing. Such responses cannot be simulated smoothly using BBM model in its original form. Although, modifications implemented to the original BBM can mimic this transition, it is abrupt. The continuous and highly non-linear stress-strain predictions of such soils could be significantly improved by incorporating within the constitutive framework the associated constitutive parameters that could be calibrated using experimental data. Researchers have to rely on scarce experimental data obtained from shear-induced un-

saturated soil response. The collected data plays a vital role in the calibration of key model parameters necessary to validate and improve the accuracy of model predictions.

2 MATERIALS AND TESTING METHODS

2.1 *Soil type and index properties*

The soil tested in current research is classified as a silty sand (55% sand, 37% silt and 8% clay) as per USCS classification. Thus, it is neither a perfect sand nor a silt but a perfect intermediate geo-material to be tested. Most of the available experimental data from past research is on silts, clays, and sands, thus necessitating increasingly experimental evidences to corroborate such response. Axis-translation technique was used to apply and control matric suction within silty sand specimens.

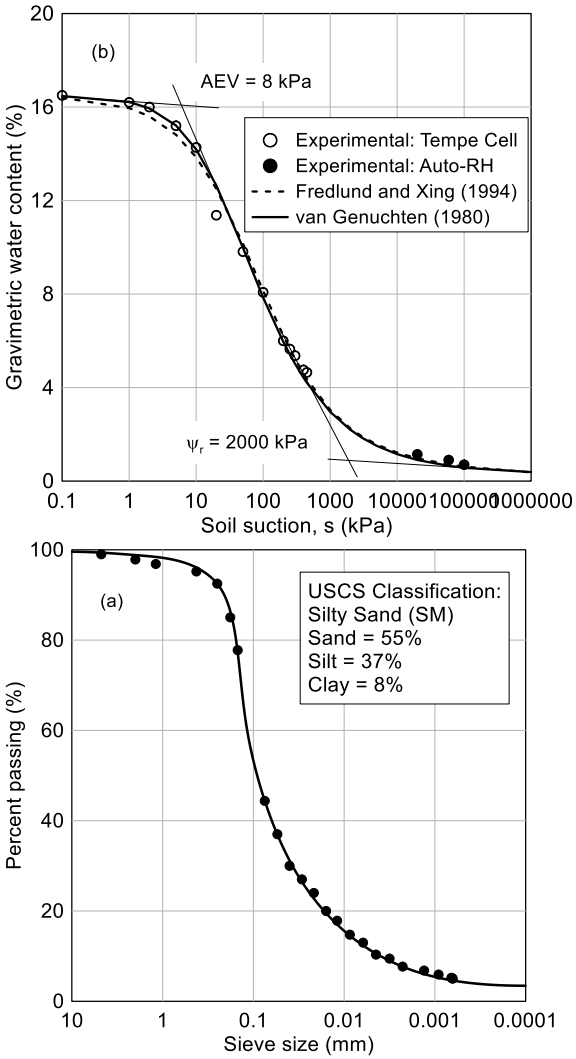

Figure 1. a) Sieve analysis of silty sand and (b) Soil water characteristic curve for compacted silty sand

Soil used in this study is classified as a silty sand as per Unified Soil Classification System (USCS). The particle size distribution and the soil water characteristic curve are as shown in Figs 1(a) and (b). Soil specimens of diameter 2.8 in. and height of 5.6 in. were prepared by static compaction method via compacting the test soil in nine equal lifts. Each lift was subjected to maximum stress of 1600 kPa to produce soil specimen with artificially induced over-consolidated stress history. The compacted soil specimens had initial voids ratio varying between 0.46-0.48 and approximate air entry value between 8-10 kPa (Patil 2014; Patil et al. 2016; Patil et al. 2017).

2.2 *Test setup and arrangement of instruments*

Suction-controlled shear strength tests were conducted using a fully-automated double-walled triaxial test equipment. This equipment was modified for unsaturated soil testing, and included high-air-entry (HAE) ceramics in the bottom pedestal; pore-water pressure control; pore-air pressure supply via the top cap; and diffused-air flushing assembly. A panoramic view of test apparatus is as illustrated in Fig. 2.

A series of saturated and unsaturated consolidated drained (CD) triaxial tests was performed on compacted specimens and the matric suction was applied and controlled using the axis-translation technique. The matric suction applied was 50 and 250 kPa and the net confining pressures, $(\sigma_3 - u_a)$ applied was 100 and 300 kPa. Furthermore, the details regarding the test procedure adopted and the capabilities of the test equipment are explained by Patil (2014) and Patil et al. (2016).

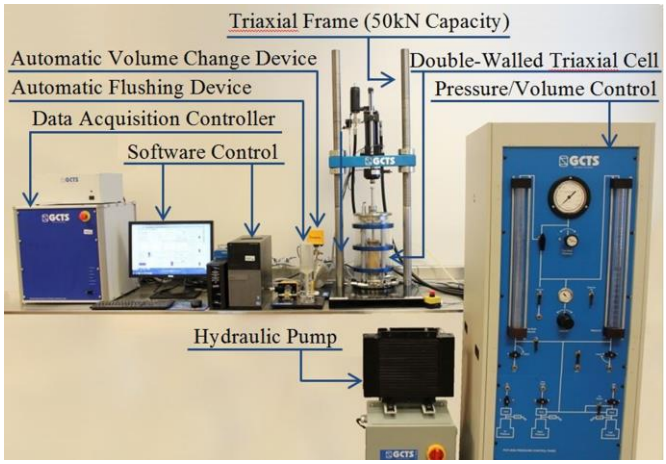

Figure 2. Panoramic view of actual unsaturated soil triaxial set up

3 EXPERIMENTAL RESPONSE OF SILTY SAND UNDER SUCTION-CONTROLLED TRIAXIAL TESTING

Test results from suction-controlled CTC (Conventional triaxial compression) tests under constant matric suction, s = 250 kPa, and under two net confining pressures, $(\sigma_3 - u_a)$ = 100 and 300 kPa, are shown in Figure 3. A negative sign in the volumetric strain response represents dilating volume change, while a positive sign indicates compressive type behavior. The convention used to designate the specimen is CDx-y where "CD" denotes the consolidated drained

test; "x" represents the net confining pressure ($\sigma_3 - u_a$), while "y" represents the imposed constant suction (s).

Experimental results showed an increase in shear strength with increasing confinement (Fig. 3a). The triaxial tests performed on saturated specimens of compacted silty sand (s = 0) resulted in strain-hardening type stress-strain response and compressive type of volumetric response. Similar response was observed by previous researchers (Russel and Khalili 2006; Cattoni et al. 2004; Hossain et al. 2010; Ng et al. 2016). However, at s = 250 kPa, the deviator stress increased with increasing axial strain up to a peak stress and thereafter, a post-peak reduction in deviator stress, also known as strain-softening type behavior, was observed (Fig. 3a).

Furthermore, an increase in net confinement pressure caused higher volumetric compression of the specimen thereby, suppressing the amount of dilation. This is clearly observed in Figure 3(b), where dilation is significantly suppressed with an increase in confining pressure from 100 to 300 kPa. The observed stress-strain and volume change response are typical of relatively dense and overconsolidated soils, as is the case of statically compacted silty sands (Russel and Khalili 2006; Yu 2006).

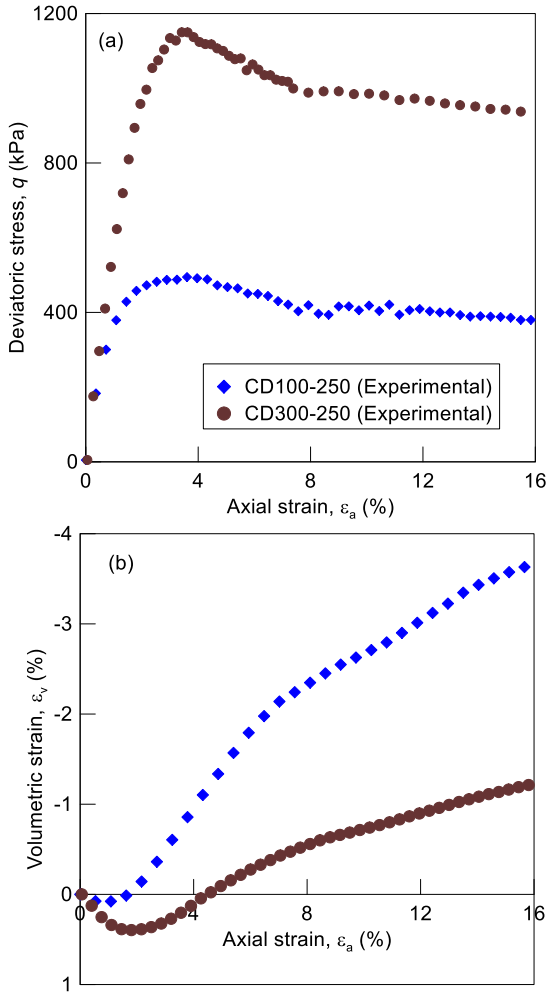

Figure 3. Response of compacted silty sand (a) Stress-strain and (b) Volumetric response.

4 CONSTITUTIVE MODELING OF OVER CONSOLIDATED SILTY SAND RESPONSE

4.1 *Bounding surface model: General framework*

The framework of the Bounding Surface Model (BSM) introduced by Morvan et al. (2010) can capture the compressive volumetric response and strain-induced hardening type response. These behaviors are typically observed in normally and lightly over-consolidated soils. However, this BSM framework also has the potential to reproduce dilational volumetric response and strain-induced softening that are typically observed in heavily overconsolidated soils subjected to suction-controlled monotonic shearing. Furthermore, it is possible with BSM to capture the gradual transition between elastic and elasto-plastic soil response.

The purpose of this study was to finetune and refine the Bounding Surface Model by Morvan et al. (2010) to predict the stress-strain and volume change response and compare it with the one obtained via suction-controlled triaxial testing from present research.

4.2 *Effective stress: definition and radial mapping*

The effective stress chosen, σ', is the simple form proposed by Bishop (Bishop 1959) and hence is given as follows:

$$\sigma' = \sigma - u_a + sS_r \qquad (1)$$

As previously mentioned, the model introduced by Morvan et al. (2010) to simulate unsaturated soil response is essentially an extension of the BS model postulated by Bardet (1986) for saturated soils, and hence is based on the bounding surface theory within a critical state framework. Therefore, due consideration is given to the existence of a limit state line (LSL) in the p', q plane that defines an upper bound to the stress ratio $\eta_p = q/p'$, as illustrated in Fig. 4. The plastic modulus is forced to be dependent on the distance δ between the current stress state σ' and its image-point, $\bar{\sigma}$ obtained by projection on the distance δ between the current stress state σ' and its image-point, obtained by projection on a surface called bounding surface, as shown in Figure 4.

Radial mapping technique Bardet (1986), also illustrated by Yu (2006), is used to define the image-point $\bar{\sigma}^r$ of the actual stress σ' on the bounding surface BS, via a translation vector, by extending the line linking the origin to the point σ' until it cuts the bounding surface (Fig. 4). Further details on the classic BS formulation have been presented by Dafalias and Herrmann (1986), Manzari and Dafalias (1997), Russell and Khalili (2006), and Yu (2006).

4.3 *BSM framework in triaxial stress space*

Classic triaxial test variables are used for cylindrical symmetry and triaxial stress space to define the mean net stress (p'), deviatoric stress (q), peak state line (PSL) slope (η_p), and critical state line (CSL) slope (M), which are expressed as follows:

$$p' = \sigma_1 + 2\sigma_3, \quad q = \sigma_1 - \sigma_3, \quad \eta_p = \frac{q_p}{p_p}, M = \frac{q_{cs}}{p_{cs}} \quad (2)$$

In this work, peak state line (PSL) is used exchangeable to limit sate line (LSL), as shown in Fig. 4. A third line, identified as the characteristic state line (CL), which marks a transition from contractant to dilatant volume change behavior during initial stages of shear loading, is also postulated.

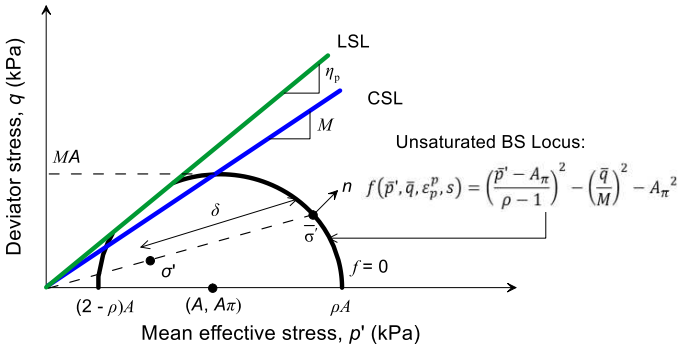

Figure 4. Radial mapping defining image point on the unsaturated bounding surface BS (modified from Bardet (1986) model)

The conjugated variables in p', q plane is volumetric and deviatoric strains, ε_p and ε_q, which are respectively defined as follows:

$$\varepsilon_p = (\varepsilon_1 + 2\varepsilon_3)/3, \quad \varepsilon_p = 2(\varepsilon_1 - \varepsilon_3)/3 \quad (3)$$

The total strain is assumed to be divided into elastic and plastic parts:

$$\varepsilon_p = \varepsilon_p^e + \varepsilon_p^p, \quad \varepsilon_q = \varepsilon_q^e + \varepsilon_q^p \quad (4)$$

The BS yield function represents an ellipse-shape yield surface in p':q plane (Fig. 4), beyond which plastic compression occurs on account of increased stress or decreased suction, and is defined as follows:

$$f(\bar{p}', \bar{q}, \varepsilon_p, s) = \left(\frac{\bar{p}' - A_\pi}{\rho - 1}\right)^2 - \left(\frac{\bar{q}}{M}\right)^2 - A_\pi{}^2 \quad (5)$$

The stress image obtained by the radial mapping, as shown in Fig. 4.

The 3 components of the exterior normal at the image-point can be expressed as follows:

$$n_p = \frac{\frac{\partial f}{\partial \bar{p}'}}{\left\| \frac{\partial f}{\partial \bar{\sigma}'} \right\|}, \quad n_q = \frac{\frac{\partial f}{\partial \bar{q}}}{\left\| \frac{\partial f}{\partial \bar{\sigma}'} \right\|}, \quad n_s = \frac{\frac{\partial f}{\partial \bar{s}}}{\left\| \frac{\partial f}{\partial \bar{\sigma}'} \right\|} \quad (6)$$

Employing the regular concept and the definitions of plastic multiplier ζ and plastic modulus H_b, the following equation can be established:

$$H_b = \frac{1 + e_0}{\lambda(s) - \kappa} \frac{Al_1}{g^2} M^2 (\gamma - 1)[\gamma + \rho(\rho - 2)] \quad (7)$$

With,

$$g = \left\| \frac{\partial f}{\partial \bar{\sigma}'} \right\| \frac{M(\rho - 1)^2}{2A_\pi} \quad (8)$$

where κ is the volumetric deformability and e_0 is the initial void ratio. If the stress point lie on the bounding surface, the plastic modulus equals H_b. On the other hand, if the stress point lie within the bounding surface, an additional term H_f is added to H_b. The plastic modulus H is then expressed as follows:

$$H = H_b + H_f \quad (9)$$

H_f is related to the plastic modulus H by the distance δ between the current stress state σ' and its projected image-point $\bar{\sigma}'$ on the bounding surface, as illustrated in Fig. 4, and is expressed as follows:

$$H_f = \frac{1 + e_0}{\lambda(s) - \kappa} \frac{\delta}{\delta_{\max} - \delta} h_0 p' \frac{\eta_p - \eta}{M} \quad (10)$$

where h_0 is a material parameter.

Inclusion of hardening of the unsaturated soil due to an increase in matric suction and plastic volumetric strains is essential for the development of a consistent hardening rule. The plastic flow is assumed to take the same direction as the onset of yielding by adopting an associative flow rule relating the incremental plastic components of volumetric and shear strains, which are expressed as follows:

$$d\varepsilon_p^p = \frac{1}{H}(n_p dp' + n_q dq + n_s ds) n_p \quad (11)$$

$$d\varepsilon_q^p = \frac{1}{H}(n_p dp' + n_q dq + n_s ds) n_q \quad (12)$$

while the elastic strains are defined by the classic relations:

$$d\varepsilon_p^e = \frac{\kappa}{1 + e_0} \frac{dp'}{p'}, \quad d\varepsilon_q^e = \frac{2(1 + \nu)}{9(1 - 2\nu)} \frac{\kappa}{1 + e_0} \frac{dq}{p'} \quad (13)$$

where ν is the poisson's ratio.

Considering the present experimental data, the suction-dependence of A_π for S_r<1 can be expressed as follows:

$$A_\pi(\varepsilon_P^P, s) = l_1(s) A(\varepsilon_P^P), \quad l_1(s) = 1 + k_1(sS_r - s_e) \quad (14)$$

where, S_r is the degree of saturation.

The slope of CSL in the e-log p' plane is assumed to be identical to that of the normal compression line (NCL) at constant suction, and is defined as follows:

$$\lambda(s) = \lambda_0 - k_3(sS_r - s_e) \quad \text{for } S_r < 1 \quad (15)$$

4.4 *Essential BSM constitutive parameters*

The modified BS model postulated in the present work requires 12 material parameters, 8 of which are necessary to define the behavior at full saturation: (1) Two elastic constants, ν and κ; (2) Six constants for plastic behavior, out of which three are required to

determine the position and the shape of the bounding surface ρ, M and A_0, two for the plastic modulus, η_p and h_0, and one for the volumetric compressibility, λ_0. Four other constants are needed to account for suction: (1) Two constants, s_e and α, to define the water retention curve, information required to determine the equivalent pore pressure so that the effective stress can be obtained; (2) One constant, k_1, to account for suction effects on the hardening parameter A_π, and (3) the last one, k_3, to define the function $\lambda(s)$.

Systematic calibration procedure was followed to extract BS model parameters for compacted silty sand from conducted experiments. More details on calibration of material properties can be obtained from Morvan et al. (2010).

5 BSM PREDICTIONS OF COMPACTED SILTY SAND RESPONSE

All the specimens were sheared along CTC stress paths.

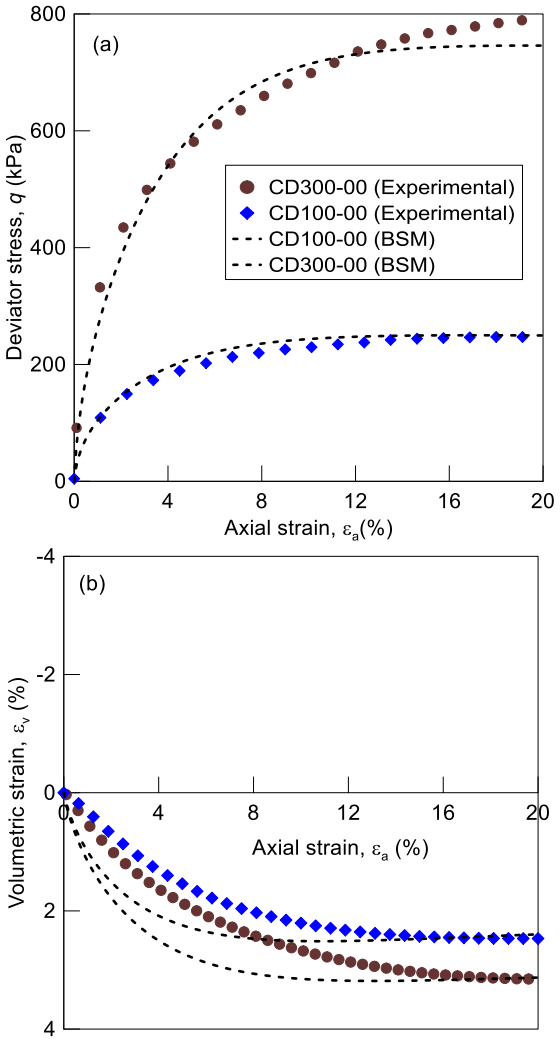

Figure 5. Experimental and BSM predictions: (a) Stress-strain and (b) Volumetric response of saturated silty sand.

Figs. 5 and 6 show comparisons between BSM predictions and experimentally observed stress-strain and volume change curves of compacted silty sand from fully drained (constant suction) CTC tests conducted at 2 different values of matric suction, s = 0 and 250 kPa, and for initial values of net mean stress, $p = (\sigma_3 - u_a)$ = 100 and 300 kPa, respectively.

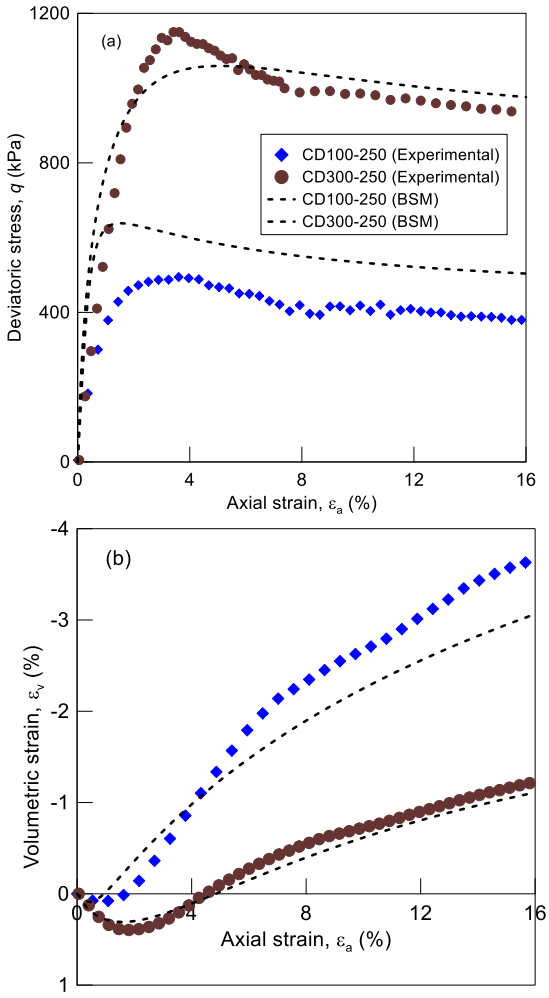

Figure 6. Experimental and BSM predictions: (a) Stress-strain and (b) Volumetric response of unsaturated silty sand at s = 250 kPa.

The BSM is able to reproduce the stress-strain and volume change response of compacted silty sand, under both saturated and unsaturated conditions, with reasonable accuracy. It is worth noting that saturated silty sand samples showed compressive type volume change response, which turned into dilating type as soon as the soil was subjected to a matric suction as low as 50 kPa. The BSM was able to capture this drastic transition in volume change quite smoothly. This transition is possible because of the term added to the plastic modulus when the stress point lies inside the surface (Eqs. 9 and 10).

On the other hand, saturated silty sand samples showed hardening type stress-strain response, which quickly changed to post-peak softening type behavior under suction-controlled conditions (s = 250 kPa).

Likewise, the BSM was able to capture this transition rather smoothly and successfully. The increase in magnitude of post-peak softening with increasing matric suction is also closely captured by the BSM, as shown in Fig. 6. This close prediction of post-peak strain softening can be attributed to the incorporation of two state lines into the BSM framework: the commonly used CSL (critical state line) and the LSL (limit state line), as shown in Fig. 4. The stress path can cross the CSL, but the LSL limits the accessible domain and whether it is crossed or not, the CSL will be the asymptote of the stress path.

Currently, the authors are investigating into experimental response at increasing suction to improvise the existing model, especially to incorporate additional parameters to reflect high suction impact on response, to enable possible better predictions. It should be noted that the soil tested in this research work was a silty sand and hence, hydraulic hysteresis effects were reasonably neglected.

6 SUMMARY AND CONCLUSIONS

Essential constitutive parameters postulated by the extended BS model framework were calibrated and used for prediction of peak deviator stress under saturated (s = 0) condition and at a matric suction of 50 and 250 kPa. The extended BS model was able to simulate the stress-strain and volume change response reasonably well as well as capture smoothly the transition of stress-strain response from strain-hardening to post-peak strain softening along with the contemporaneous transition of volume change from compressive to dilatant type on account of suction with reasonably well captured simulations. With additional testing in future, the current version of generalized BS model framework could be further generalized and made more flexible to accommodate experimental response from more soil types with broader suction range.

7 ACKNOWLEDGEMENTS

Experimental work described in this paper is funded by the National Science Foundation under MRI Award No. 1039956. This support is gratefully acknowledged. Any findings, conclusions, or recommendations expressed in this material are those of the authors and do not necessarily reflect the views of the National Science Foundation.

8 REFERENCES

Alonso, E.E., Gens, A. & Josa, A.A. 1990. Constitutive model for partially saturated soils. *Géotechnique* 40(3): 405-430.

Bardet, J.P. 1986. Bounding surface plasticity model for sands. *Journal of Engineering Mechanics* 112(11): 1198-1217.

Bishop, A.W. 1959. The principle of effective stress. *Tecknish. Ukebland* 106(39): 859-863.

Cattoni, E., Cecconi, M. & Pane, V. 2004. An experimental study on a partially saturated pyroclastic soil: the Pozzolana Nera from Roma. *Proceedings of The Second Workshop on Unsaturated Soils* Tarantino and Mancuso (eds), Capri: Italy, 29-42.

Dafalias, Y.F. & Herrmann, L.R. 1986. Bounding surface plasticity: II. Application to isotropic cohesive soils. *Journal of Engineering Mechanics* 112(12): 1263-1291.

Fredlund, D.G. & Morgenstern, N.R. 1977. Stress strain variables for unsaturated soils. *Proceedings of American Society of Civil Engineering* 103(GT5): 447-466.

Hilf, J.W. 1956. An investigation of pore water pressures in compacted cohesive soils. *U.S. Department. of the interior, Bureau of Reclamation Tech. Memo* 654, Denver, Col., U.S.A.

Hossain, M.A. & Yin J.H. 2010. Shear strength and dilative characteristics of an unsaturated compacted completely decomposed granite soil. *Canadian Geotechnical Journal* 47(10): 1112-1126.

Jennings, J.E. & Burland, J.B. 1962. Limitations to the use of effective stresses in partly saturated soils. *Geotechnique* 12(2): 125-144.

Karube, D. 1988. New concept of effective stress in unsaturated soil and its proving test. *In Advanced triaxial testing of soil and rock. ASTM* SPT No. 977: 539–552.

Khalili, N. & Khabbaz, M.H. 1998. A unique relationship for the determination of the shear strength of unsaturated soils. *Geotechnique* 48(5): 681-687.

Kohgo, Y., Nakano, M. & Miyazaki, T. 1993. Theoretical aspects of constitutive modeling for unsaturated soils. *Soils and Foundations* 33(4): 49-63.

Lu, N. & Likos, W.J. 2006. Suction stress characteristic curve for unsaturated soil. *Journal of Geotechnical and Geoenvironmental Engineering* 132(2): 131-142.

Manzari M.T. & Dafalias Y.F. 1997. A critical state two-surface plasticity model for sands. *Geotechnique* 47(2): 255-272.

Matyas, E.L. & Radhakrishna, H.S. 1968. Volume change characteristics of partially saturated soil. *Géotechnique* 18(4): 432-448.

Morvan, M., Wong, H. & Branque, D. 2010. An unsaturated soil model with minimal number of parameters based on bounding surface plasticity. *International Journal for Numerical and Analytical Methods in Geomechanics* 34: 1512-1537.

Ng, C.W.W., Sadeghi, H. & Jafarzadeh, F. 2016. Compression and shear strength characteristics of compacted loess at high suctions. *Canadian Geotechnical Journal* 54: 690-699.

Patil, U.D. 2014. Response of unsaturated silty sand over a wider range of suction states using a novel double-walled triaxial testing system. *Ph.D. dissertation, Univ. of Texas at Arlington, Arlington, TX.*

Patil, U.D., Hoyos, L.R. & Puppala, A.J. 2016. Modeling essential elasto-plastic features of compacted silty sand via suction-controlled triaxial testing. *International Journal of Geomechanics* 16(6), DOI: 10.1061/(ASCE)GM.-1943-5622.0000726.

Patil, U.D., Puppala, A.J., Hoyos, L.R. & Pedarla, A. 2017. Modeling critical-state shear strength behavior of compacted silty sand via suction-controlled triaxial testing. *Engineering Geology* 231: 21-33.

Russel, A.R. & Khalili N. 2006. A unified bounding surface plasticity model for unsaturated soils. *International Journal for Numerical and Analytical Methods in Geomechanics* 30(3): 181-212.

Yu, H.S. 2006. Plasticity and geotechnics. *Springer*: New York.